Computational investigation of transport parameters of ions in gas-filled radiation detectors

Yalçın Kalkan [ID],[a,b,d,e,*] **Sedat Arı** [ID],[a,d] **Salim Orak** [ID][c] **and Rob Veenhof** [ID][d]

[a]*Nuclear Radiation Detectors Application and Research Center, Bolu Abant İzzet Baysal University, Bolu, Türkiye*

[b]*Mehmet Tanrıkulu Vocational School of Health Services, Bolu Abant İzzet Baysal University, Bolu,Türkiye*

[c]*University of Health Sciences, Hamidiye Vocational School of Health Services, İstanbul, Türkiye*

[d]*CERN, CH-1211, Geneva 23, Switzerland*

[e]*Department of Detector and Sensor Technologies, Muş Alparslan University, Muş, Türkiye*

E-mail: yalcin.kalkan@ibu.edu.tr

ABSTRACT: In this study, a novel computational method was developed to investigate the transport characteristics of ions in gas-filled radiation detectors, which are closely linked to the behavior of ions in gaseous detectors. Parameters such as polarizability, mean free path, collision frequency, and mean free time, which directly impact ion mobility, were physically manipulated using the Monte Carlo technique, and the results were validated against fundamental physical principles. As an initial scenario, computations were performed on the mobility of Ar^+ ions in an argon environment as a carrier gas. The distribution of the radial velocity components of the ion following an ion-gas collision was represented as a two-dimensional histogram with a disc-shaped pattern, and this result was elucidated utilizing the Maxwell-Boltzmann distribution. The findings regarding the mean free time and mean free path of an Ar^+ ion in an argon carrier gas align with the results derived from Skullerud's methodologies. These findings hold promise for Garfield^{++} simulations, enabling the computation of ion mobility and even cluster ions in the mixture, thereby considering their impact on the detector's gain parameters. The results of this investigation offer novel insights into the behavior of ions within detector settings, significantly enhancing our comprehension of the mobility of ions and its effects on radiation detection efficiency.

---

*Corresponding author.

Contents

1 Introduction

The advancement in particle physics is closely linked to the continuous development of radiation detector technologies. Resolving the issues associated with detectors is crucial to promote research in existing accelerator facilities [1]. Gaseous radiation detectors have extensive applications in various industries, including accelerators, nuclear and hadron physics experiments, astroparticle physics and neutrino experiments, medical imaging, materials science, and security applications [2, 3]. A common challenge with these detectors is the presence of ions within the detector volume, which can persist for extended periods and disrupt the electric field configuration due to their limited mobility [4–6]. Therefore, it is essential to understand the impact of ions on the operation of gaseous radiation detectors while considering the diffusion and mobility parameters. These parameters are even more significant when clusters, rather than individual ions, serve as actual signal ions [7].

The positive ion, created by radiation in the drift region of a gas-filled radiation detector, is given kinetic energy by the electric field. Occasionally, it may lose energy through collisions with neutral gas atoms or molecules. When the system is in equilibrium, the average velocity of the ion, v_d, or the drift velocity, is proportional to the strength of the electric field, E, in the drift region. This can be expressed mathematically as in equation 1.1 [6]:

$$v_d = K \cdot E \tag{1.1}$$

The mobility of the ions, K, and the intensity of the electric field applied to the drift area of the detector are used in many applications. Reduced ion mobility, K_0, is also often mentioned in the literature [5].

$$K_0 = \frac{K \cdot N}{N_0} \tag{1.2}$$

The gas number density, N, is generally expressed in terms of the Loschmidt number, N_0, which is equal to $2.6867 \times 10^{25}\,\mathrm{m}^{-3}$. The Townsend unit is used to measure the reduced electric field, with $1\,\mathrm{Td}$ equivalent to $10^{-21}\,\mathrm{V} \cdot \mathrm{m}^2$.

The mobility of ions in gas mixtures, particularly in the context of gaseous radiation detectors, has been investigated through various experiments. Cortez et al. made a significant contribution to this field by using a gas electron multiplier (GEM) foil to measure the mobility of ions in gas mixtures [8–11]. Dwivedi et al. used chiral ion mobility spectrometry (CIMS) to measure the mobility parameters of different ionic structures, including pharmaceuticals, amino acids, and carbohydrates, providing valuable information on ion mobility [12]. Ellis et al. conducted a comprehensive study that is widely regarded a key reference in the literature, examining the mobility of ions in gas volumes and presenting important findings [13–16].

Deisting et al. conducted ion mobility measurements in gases commonly used in gas detectors as part of an effort to upgrade the ALICE Time Projection Chamber (TPC) detector at CERN [17]. Wyttenbach et al. provided a theoretical basis for ion mobility experiments, presenting a compilation of concepts and methods used in this field, along with some applications found in the literature [18]. Marrero and Mason published extensive data on gaseous diffusion coefficients under various conditions, which contributed to understanding the diffusion of ions in gases [19]. Previous sources, such as the International Critical Tables, Landolt Bornstein Tables, and Thermophysical Properties Research Literature Retrieval Guide, have presented limited catalogs of measured diffusion coefficients [20–22]. Furthermore, several reviews have provided information on specific aspects of ion mobility and diffusion, further improving the available literature [23–30].

This research incorporates theoretical deductions to develop a novel computer model aimed at simulating the movement characteristics of ions or cluster ions in a gas-filled radiation detector. These characteristics include polarizability, mean free path, collision frequency, and mean free time. The evaluation of the outcomes derived from the theoretical modeling, which is grounded on fundamental principles and implemented using ROOT [44], is also encompassed. The findings of this investigation could potentially revolutionize the development and operation of negative-ion drift detectors, particularly Time Projection Chambers (TPCs) [51, 52]. These detectors are essential in diverse scientific domains like particle physics, nuclear physics, and astrophysics, as they facilitate precise tracking and identification of charged particles. It is important to highlight that Skullerud's model serves as the primary foundation of this study, with the subsequent theories forming the fundamental principles on which the Skullerud Model relies. A comprehensive understanding of these theories is imperative for accomplishing the study's objectives.

1.1 Langevin Theory

The Langevin Theory is presented as a fundamental idea for ion mobility in low-strength electric fields. According to Langevin theory [32], when the hard-sphere repulsion is insignificant compared

to the polarization effect, the reduced mobility reaches its ultimate value. This limit is expressed in units of $cm^2 V^{-1} s^1$ and can be calculated using the following equation.

$$K_0 = 13.88 \cdot \left(\frac{1}{\alpha \cdot \mu}\right)^{\frac{1}{2}} \tag{1.3}$$

The neutral polarizability (α) of Ar and CO_2 is 1.64 and 2.613 cubic angstroms, respectively, as reported in [33] and [34] and μ is the ion-neutral reduced mass in units of atomic mass. The Langevin limit is the value of K_0 when both the ratio of electric field to particle number density and the temperature are low, making the polarization attraction more influential than the hard-sphere repulsion.

Langevin theory provides insight into the mechanisms that control ion mobility in the gas phase when exposed to weak electric fields. It is a useful addition to earlier theories, which were limited in their applicability to small electric field strengths and could not accurately capture the complexities of the physical process in question.

1.2 Mason-Shamp Theory

The Mason-Shamp Theory is analyzed to clarify the transfer of energy in ion-molecule collisions and is crucial for comprehending interactions between ions and molecules, especially in the realm of gas-phase chemistry. Introduced by Mason and Schamp in the mid-1900s, this theory offers a detailed explanation of the energy transfer mechanisms that take place when ions collide with neutral molecules [35].

According to the Mason-Schamp theory, the efficiency of energy transfer during ion-molecule collisions is predominantly influenced by the mass ratio of the colliding entities and their relative approach speed. This theory proposes that energy transfer is more effective when the ion and molecule have similar masses, leading to more efficient collisions [36]. In the context of ion-molecule interactions, a potential function is formulated, incorporating a fourth-order attraction component and a hard-sphere repulsion component. Moreover, the same attractive component is combined with an eighth-order repulsion component. The fourth-order attraction component is derived from a theoretical framework that takes into account the interplay between the ion's charge and dipole interactions. Experimental findings on the repulsion components suggest that the model based on hard-sphere repulsion demonstrates particular robustness when the impact of the eighth-order term is reduced.

In this theoretical structure, a tensile potential is created using fourth- and sixth-order terms. Additionally, considering the transfer parameters of the gases, it is expected that the repulsion potential would have a less powerful effect than the hard-sphere model, but a more powerful effect than the eighth-order term. Therefore, it was concluded that including a twelfth order term would be suitable for the repulsion potential.

1.3 Hard-sphere Model

The Hard-sphere Model assumes that ions and gas particles are rigid spheres. Mason and McDaniel studied the average energy of the ion, which can be used to measure the effective temperature (T_{eff}) and the random kinetic energies of the ion [37]. This evaluation takes into account the scattering probability of the ion in all directions in the center-of-mass frame. The contributions of thermal mobility and the external electric field can be expressed through the following equation.

$$\frac{3k_B T_{eff}}{2} = \frac{3k_B T}{2} + \overline{m_g V^2} \tag{1.4}$$

where k_B is the Boltzmann constant, T is the temperature, m_g mass of the gas atom or molecule, V is the velocity of the gas atom or molecule. It is common to encounter the following equation for the mobility of an ion in a gas environment when in thermal equilibrium [38–40].

$$K = \left(\frac{3e}{16N}\right)\sqrt{\frac{2\pi}{\mu k_B T_{eff}}}\left[\frac{(1+\Gamma)}{\Omega_D\left(T_{eff}\right)}\right] \tag{1.5}$$

In view of the association between mobility and speed, the following equation is employed to measure mobility.

$$K = \left(\frac{3e}{16N}\right)\sqrt{\frac{2\pi}{\mu k_B T_{eff}}}\left[\frac{1}{\Omega_D}\right] \tag{1.6}$$

The elastic collision cross section Ω_D, the reduced mass μ, and the correction factor Γ are all components of the equation that explains the mobility of an ion in a neutral gas medium (equation 1.4 and equation 1.6). The total momentum transfer, as reported in the literature [41], is the foundation of these equations. When experimental data are collected, there are several factors that can limit the results, such as the charge of the electron (e), the mobility (K) and the number of atoms per unit volume (N). It is known to have an inverse relationship with the gas density for a given effective temperature value. The drift velocity of ions, at a given temperature, is based on both their mobility and the effective temperature, as well as on the reduced electric field value. The existing literature reveals the use of specialized MATLAB scripts [42] to determine these dependencies. An assumption is made about the perfect symmetry of the system [38]. The code developed for simulating ion mobility in gas mixtures is based on the "Hard Sphere Model." Taking into account the information mentioned above, we can conclude that this choice is appropriate.

1.4   Null collision model

Null-Collision Model is introduced as an innovative method to model ion-gas interactions with higher precision. In this study, two simulation models were created to explain the mobility of ions in different physical states in a gas medium. However, the output of this simulation only gave the ion's velocity after a single collision. To take into account the multiple scatterings that an ion can experience before reaching the cathode, a function was added to the simulation code. This function was used to calculate the time it takes for the ion to reach the cathode because of these cumulative collisions. Using this improved simulation, the mobility of the ion was determined, and the accuracy of the models was evaluated by comparing the results with known electric field conditions.

The movement of an ion in a gas medium is not continuous but rather sporadic because of its inertial mass. As a result, the ion moves by jumping between gas atoms, resulting in an irregular path. Although the ion generally moves in the direction of the electric field, its progress towards the cathode may not always be steady. In some cases, the ion may even be reflected in the opposite direction. To gain a better understanding of ion behavior in a gas environment, it is important to consider physical quantities such as the ion's trajectory in a constant electric field, the time taken to reach the cathode, and the total number of collisions encountered along its path. These quantities can provide valuable insights into the ion dynamics in gas and help explain the sequence of events.

The frequency of collisions between an ion and gas atoms in a gas environment depends on various factors such as the ion's velocity, gas density, and cross-section. Additionally, the number of

gas atoms is influenced by the temperature and pressure of the gas. It can be challenging to calculate a complex physical event that involves multiple parameters. In 1968, Skullerud developed a model to determine the duration for which an ion can travel without experiencing a collision. Furthermore, he proposed an algorithm, based on certain concepts, to address this problem [46]. The average collision frequency of an ion ($\nu(v)$) with an initial velocity v_i can be represented as:

$$\nu(v) = N v_i \sigma(v) \tag{1.7}$$

The number of gas atoms per unit volume is represented by N, while the velocity of the ion is indicated by v. The collision cross section is defined as $\sigma(v)$. The ion experiences continuous acceleration due to the electric field, which is represented by a. The alteration in velocity can be basically expressed in the following manner.

$$v = v_i + at \tag{1.8}$$

The path of the ion's motion is parabolic as a result of the acceleration. For the interval of $[0, \tau]$ time, the probability that the real duration of free time (without any collision) is higher than the average duration of free time can be represented as

$$P(t) = \exp\left(-\int_{t=0}^{\tau} \nu(|v_i + at|)dt\right) \tag{1.9}$$

The computer is able to produce a uniformly distributed random number S between 0 and 1.

$$P(t) = S \tag{1.10}$$

A computer simulation that is based on a collision frequency that is not dependent on velocity can help to overcome the restrictions on the number and magnitude of collisions. This would make the simulation process more manageable and efficient.

By solving the equations together to find the value of τ, the following expression is obtained:

$$\tau = \nu^{-1} \log S \tag{1.11}$$

Additionally, the number of collisions that will take place within the period $[0, \tau]$ can be easily expressed as:

$$\Pi = \int_0^{\tau} \nu(t)dt \tag{1.12}$$

The number of collisions that occur within a certain time period τ follows an exponential distribution. This type of distribution is often used to represent events that are not affected by previous events. However, it is important to consider whether Sklerrud's equation [46], which is the basis of this research, is suitable for the physical event being studied. After careful consideration, it is clear that the number of collisions within a given time τ is not necessarily determined by the number of collisions the ion has experienced before that time. Consequently, equation 1.7 can be used to address this issue.

2 Material and Methods

2.1 Ion-gas Interactions

To understand the effect of ions or cluster ions on the signal generation of gas-filled radiation detectors, it is essential to comprehend the interactions between ions, ion-neutral gas atoms/molecules, and ions with the internal components of the detector. These interactions can usually be approximated as elastic collisions. During an elastic collision between an ion and a gas atom in the detector, momentum and kinetic energy are conserved.

Before collision, an ion with velocity $v(v_x, v_y, v_z)$ and a gas atom/molecule with velocity $w(w_x, w_y, w_z)$ approach each other. The velocities after collision are $V(V_x, V_y, V_z)$ and $W(W_x, W_y, W_z)$, respectively. As a general expression for momentum conservation during collision, the following equation can be written:

$$m_i \sqrt{v_x^2 + v_y^2 + v_z^2} + m_g \sqrt{2E_k} \cos b = m_i \sqrt{V_x^2 + V_y^2 + V_z^2} + m_g \sqrt{W_x^2 + W_y^2 + W_z^2} \qquad (2.1)$$

In this situation, E_k stands for the kinetic energy of the gas atom before collision, m_i is the mass of the ion, m_g is the mass of the gas atom or molecule, and b is the impact parameter for the particular collision (see figure 1). It is possible to express momentum conservation equations in three directions: x, y, and z.

$$m_i v_x + m_g w_x = m_i V_x + m_g W_x$$
$$m_i v_y + m_g w_y = m_i V_y + m_g W_y$$
$$m_i v_z + m_g w_z = m_i V_z + m_g W_z$$

Given that the collision is expected to happen in two dimensions, it is evident that only a pair of these equations can be utilized to determine the unknowns. The conservation of kinetic energy equation is essential for determining the ion's momentum components along all three axes following the collision.

$$\frac{1}{2} m_i v^2 + \frac{1}{2} m_g w^2 = \frac{1}{2} m_i V^2 + \frac{1}{2} m_g W^2 \qquad (2.2)$$

The range of values for the impact parameter can be established in this collision. When the ion strikes the gas molecule directly (head-on collision), the impact parameter is zero ($b = 0$). However, when the ion collides tangentially with the gas molecule, the impact parameter reaches its highest value. Thus, the limits of the impact parameter can be expressed as follows.
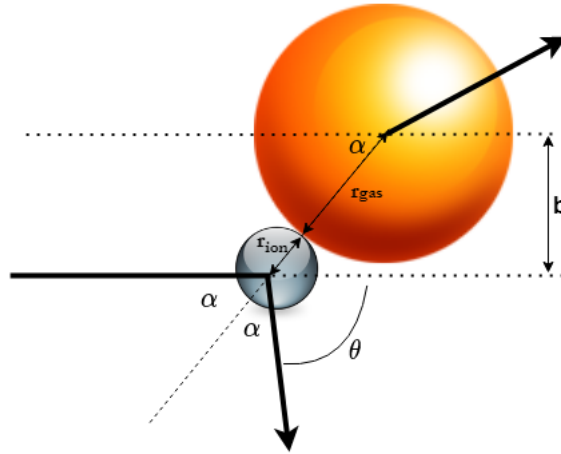
$$0 \le b \le r_{\text{gas}} + r_{\text{ion}} \qquad (2.3)$$

To simplify ion-gas collisions, it is beneficial to consider the center-of-mass frame. To perform this transformation, the velocity of the center of mass must be calculated. This can be accomplished by following the steps described below.

$$\sum P = m_i v_i + m_g v_g \ne 0 \qquad (2.4)$$

$$\sum P_{\text{CM}} = m_i (v_i + v_{\text{CM}}) + m_g (v_g + v_{\text{CM}}) = 0 \qquad (2.5)$$

$$v_{\text{CM}} = -\frac{m_i v_i + m_g v_g}{m_i + m_g} \qquad (2.6)$$

Figure 1. Representation of collision of ion and gas atom.

The momentum of the center of mass (P_{CM}) is assumed to be zero during the shift to the center of mass frame during collision.

Following a collision, the ion and the gas atom are scattered with the same momentum in opposite directions, creating an angle θ in comparison to their original trajectories.

$$\underbrace{m_i v_1 + m_g w_2}_{0} = m_i v \cos\theta + m_g W \cos\theta \tag{2.7}$$

Two equations of momentum conservation that must be solved in the center-of-mass frame are expressed as follows under the presumption that the impact occurs in the *x-y* plane.

$$m_i V_x + m_g W_x = 0$$
$$m_i V_y + m_g W_y = 0 \tag{2.8}$$

It is essential to recall that the collision can take place in any plane formed by two of the three axes. Consequently, it is not feasible to construct a conservation of momentum equation for one of the axes. Since energy is a scalar quantity, the conservation of the energy equation remains unchanged.

$$m_i \, |v| = m_g \, |w|$$
$$m_i \, |V| = m_g \, |W|$$
$$|v| = \frac{m_g \, |w|}{m_i}$$
$$|V| = \frac{m_g \, |W|}{m_i}$$

The orientation and speed of the velocities of the ion and gas atoms play a crucial role in determining the chances of a collision or interaction, as illustrated in figure 1. If the ion and gas atoms move in the same direction and the gas's thermal velocity exceeds that of the ion, the likelihood of a collision or interaction decreases significantly. Conversely, when the velocity vectors of the ion and gas are opposite before collision, the probability of interaction increases. This is where

statistical computations come into play. In a one-dimensional scenario, collisions are ruled out when the ion and gas velocities are equal and in the same direction. To tackle this issue, the absolute value function was employed, enabling the resolution of this problem in one dimension by expressing the gas velocity distribution for collision cases as follows:

$$f(w) = \left(\frac{m_g}{2\pi k_{\mathrm{B}}T}\right)^3 4\pi |W - v| e^{-\frac{m_g v^2}{2k_{\mathrm{B}}T}} \tag{2.9}$$

This result obtained with the Monte Carlo method derived can also be mathematically validated briefly. Given an ion moving at constant speed through gas atoms arranged along a linear path and possessing velocities following the Maxwell distribution, the initial step involves performing statistics to determine which gas atom it will interact with. The focus is on the likelihood of collision, which is influenced by factors like the positions of the ion and gas atoms, as well as the magnitudes and directions of their velocities. Rather than relying on the simplistic statistical scenarios mentioned earlier, it is essential to consider velocity distributions. Consequently, the objective is to establish a distribution for the ion's or ionic cluster's free-flight time. Furthermore, the velocity of the ion following each elastic collision can be determined by applying the principles of momentum conservation. Nevertheless, it has been noted that the Maxwell distribution alone is inadequate to characterize the velocities of gas atoms or molecules within the medium. This is because the gas molecules exhibit nonuniform motion in terms of direction and speed, and these factors significantly impact the probability of collision.

To obtain a probability distribution for the unobstructed movement time of an ion starting at $x = 0$ in a one-dimensional phase space, the Delta function can be employed to express the combined velocity distributions of the gas atoms denoted as k and l, traveling at their respective thermal speeds, such that $f(x) = f(k) + f(l)$.

$$\int_{-\infty}^{+\infty} dl \int_{-\infty}^{+\infty} dk f(l) f(k) \delta(k + l - x) = f(x) \tag{2.10}$$

Eliminating the delta function yields a result similar to the following.

$$= -\int_{-\infty}^{+\infty} dl f(l) f(x - l) \tag{2.11}$$

The result agrees with the definition of the convolution integral. If we take two gas atoms with positions x_1 and x_2 and velocities v_1 and v_2, the time gaps between their collisions with the ion can be expressed as:

$$\tau_1 = -\frac{x_1}{v_1}, \qquad \tau_2 = -\frac{x_2}{v_2}$$

To comprehend the reasons behind the negative values of the expressions, one can refer to the subsequent equations, keeping in mind that the ion's position and initial velocity are both zero.

$$x_{\mathrm{ion}} + \tau_1 v_{\mathrm{ion}} = x_1 + \tau_1 v_1$$
$$x_{\mathrm{ion}} + \tau_2 v_{\mathrm{ion}} = x_2 + \tau_2 v_2$$

Therefore, the duration between the gas atom collisions that will reach the ion initially can be determined using the subsequent equation.

$$\int_{-\infty}^{+\infty} dx_1 \int_{-\infty}^{+\infty} dv_l \int_{-\infty}^{+\infty} dx_2 \int_{-\infty}^{+\infty} dv_2 f(x_1) f(v_1) f(x_2) f(v_2) \delta\left(\frac{x}{\mathrm{w}} - \left(\frac{x_1}{v_1}, \frac{x_2}{v_2}\right)\right) \tag{2.12}$$

The integral yields the magnitude of the gas velocity |w|, a key observation. The results of the Monte Carlo method are consistent with the validated mathematical analysis. However, by extending this computation to three dimensions, the concept of cross-sectional area gains importance. In collisions involving multiple dimensions, the cross section serves as a critical physical parameter.

2.2 Polarizability effect

In the context of gaseous radiation detectors, a combination of noble gas and molecular gas, referred to as the "Quencher Gas," is utilized to decrease the occurrence of photon feedback [43]. The inclusion of the molecular gas significantly affects the potential interactions between ions and molecules, primarily because of its polarizability. When the molecular gas becomes polarized, the collision between the ion and the molecule does not occur in an elastic manner; instead, they orbit around each other before eventually scattering in opposite directions. Importantly, this process does not involve any changes in momentum. This section focuses on the mathematical analysis of how polarizability impacts ion-molecule interactions.

The gain of an understanding of the polarization effect requires the estimation of the average distance between atoms in a gas. This will enable us to evaluate the alterations in the electromagnetic force and electric field and their effect on the process. The Loschmidt number indicates that in a $1\,cm^3$ gas volume, there are approximately 2.7×10^{19} atoms. Taking the cube root of this figure gives us an estimate of the distance between atoms or molecules in nanometers. This rough calculation implies that the ion and the gas atom or molecule are separated by a similar distance.

The electric field strength is directly proportional to the charge of the ion, represented as q, and inversely proportional to the square of the distance between them, represented as $\frac{1}{r^2}$. To further illustrate this concept, a calculation was performed using a polarizable molecule, such as methane and argon, a common noble gas, in the detector. The average radius of an argon atom was assumed to be approximately $70\,pm$, while the average radius of a methane molecule is around $200\,pm$. As expected, the presence of the ion induces polarization in the molecule, resulting in the formation of a Coulomb field between them. Consequently, the force between the ion and the molecule is inversely proportional to the square of the distance between them, denoted $\frac{1}{r^2}$. Regarding the electric field, its magnitude is directly proportional to the charge of the ion, represented as q, and inversely proportional to the square of the distance between them, represented as $\frac{1}{r^2}$.

$$E \propto \frac{1}{(r + \epsilon)^2} - \frac{1}{(r - \epsilon)^2} \propto \frac{-4\epsilon}{r^3} \tag{2.13}$$

In this scenario, the parameter ϵ can be disregarded as it is not significant compared to the gap between the ion and the molecule. Considering that the electromagnetic force is directly proportional to the electric field, it can be inferred that the electric force will vary with $\frac{1}{r^3}$ instead of $\frac{1}{r^2}$. It is important to note that the interaction between the ion and a gas atom or molecule that cannot be polarized by the ion differs from the interaction with a molecule that can be polarized due to the presence of the ion. The dipole moment (μ) is directly proportional to the electric field and, consequently, to the electric force.

$$F = q \cdot E = q \cdot \frac{\mu}{r^3} \tag{2.14}$$

In addition, it is basically known that;

$$\mu \propto E \propto \frac{1}{r^2} \tag{2.15}$$

The polarizability coefficient (α) can be used to illustrate the connection between two entities.

$$\mu = \alpha \cdot E = \alpha \frac{1}{r^2} \tag{2.16}$$

The electrical attraction between the ion and the dipole moment can be expressed as follows:

$$F = \frac{q \cdot \mu}{r^3} = \frac{q \cdot \alpha}{r^5} \tag{2.17}$$

It can be deduced from the evidence and arguments presented that, when an ion and a gas molecule interact, polarization occurs, leading to a swirling motion between them. This causes them to be scattered in the same or opposite directions without altering their momentum. Consequently, using molecular gases that possess natural self-polarizability, which eliminates the need for an ion to be close for polarization, is not suitable for gaseous radiation detectors.

2.3 Generating random numbers

2.3.1 Impact parameter

The impact parameter ranges from 0 to the combined radii of the gas and the ion. Taking into account the normalization condition, the normalization coefficient can be determined.
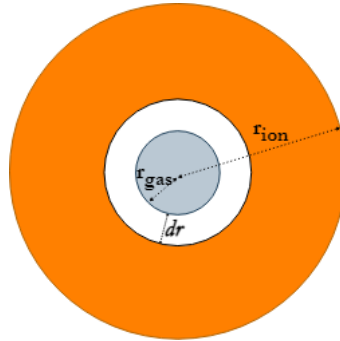
$$\int_0^{r_g+r_i} f(r)dr = c \int_0^{r_g+r_i} 2\pi r dr = 1 \qquad c = \frac{1}{\pi(r_g+r_i)^2} \tag{2.18}$$

Taking into account a limited radius (dr) and performing the necessary computations, we get the following equation; see figure 2.

$$\pi(r+dr)^2 - \pi r^2 = 2\pi r dr$$

We determined the probability density function for the impact parameter by our calculations.

$$f(r) = \frac{2\pi r}{\pi(r_g+r_i)^2} = \frac{2r}{(r_g+r_i)^2} \tag{2.19}$$
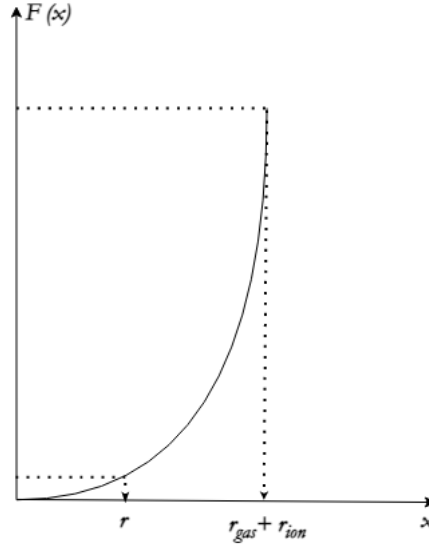

Figure 2. Diagram of the method used to generate random numbers for the impact parameter.

Accordingly, the cumulative function is obtained as follows:

$$\begin{aligned} F(x) &= \int_0^x f(r)dr \\ &= \int_0^x \frac{2r}{(r_g+r_i)^2}dr \\ &= \frac{x^2}{(r_g+r_i)^2} \end{aligned} \tag{2.20}$$

The cumulative function u produces a random number x to be used for the impact parameter, expressed as:

$$u = F(x) = \frac{x^2}{(r_g + r_i)^2} \qquad x = \sqrt{u}(r_g + r_i) \tag{2.21}$$

Figure 3. Cumulative intensity function for the impact parameter.

The effect parameter can be assigned random numbers using the following process.

$$b = \sqrt{\text{grandom} \to \text{uniform}(0, 1)}(r_g + r_i)$$

The ROOT line [44] is a result of this. It can be shown that the sizes of the ion or gas radii have no influence on the impact parameter. By incorporating the total radius R into equation (2.26), the following equation is obtained.

$$\sin \frac{\pi - \theta}{2} = \frac{b}{R} \tag{2.22}$$

Therefore,

$$\cos \frac{\theta}{2} = \frac{b}{R} \tag{2.23}$$

The following equations can be expressed using trigonometric principles.

$$\cos(2\theta) = \cos^2(\theta) - \sin^2(\theta) \tag{2.24}$$

$$\cos(\theta) = 2\cos^2 \frac{\theta}{2} - 1 \tag{2.25}$$

Using equations 2.21, equation 2.23, and equation 2.25, it can be demonstrated that the distribution of $\cos\theta$ is even across the range [0,1], regardless of the radii of the ion and gas.

2.3.2 Scattering angle

The rotation of the axes when an ion interacts with a gas molecule can be determined by computing the scattering angle (θ). As illustrated in figure 1, the following equations have been developed to calculate this angle.

$$\sin \alpha = \frac{b}{r_g + r_i} \tag{2.26}$$

$$\cos \alpha = \frac{\sqrt{(r_g + r_i)^2 - b^2}}{(r_g + r_i)} \tag{2.27}$$

$$\sin \theta = \sin 2\alpha = 2 \sin \alpha \cos \alpha \tag{2.28}$$

$$\sin \theta = 2b \, \frac{\sqrt{(r_g + r_i)^2 - b^2}}{(r_g + r_i)} \tag{2.29}$$

2.3.3 Azimuthal angle

When an ion and a gas molecule collide elastically, there is no specific physical law that determines the random selection of the azimuthal angle. This angle can take any value between 0 and 2π, so no additional laws of physics are required to assign random numbers to it [47, 48].

$$\text{phi} = \text{gRandom} \rightarrow \text{Uniform}(0, 2*\text{TMath} :: \text{Pi}())$$

It is sufficient to type a command line in ROOT.

2.4 Rotation of the ion's velocity vector and rotation vectors

The velocity of the ion in the Cartesian coordinate system can be expressed as the following components.

$$v_x = |v| \cos \theta \tag{2.30}$$

$$v_y = |v| \sin \theta \sin \varphi \tag{2.31}$$

$$v_z = |v| \sin \theta \cos \phi \tag{2.32}$$

To examine the elastic collision between the ion and the gas atom, we used the center of mass for simplicity. To do this, the velocity vector of the ion was rotated along a single axis with the help of rotation matrices. For example, consider the transformation matrix needed to represent rotation by an angle of α in the x-y plane.

$$\textbf{ROT1} = \begin{pmatrix} \cos \alpha & 0 & -\sin \alpha \\ 0 & 1 & 0 \\ -\sin \alpha & 0 & \cos \alpha \end{pmatrix} \tag{2.33}$$

The transformation matrix that must be applied to the x-axis when rotating it around the z-axis by β is expressed as follows:

$$\textbf{ROT2} = \begin{pmatrix} \cos \beta & \sin \beta & 0 \\ -\sin \beta & \cos \beta & 0 \\ 0 & 0 & 1 \end{pmatrix} \tag{2.34}$$

These operations can make the problem much simpler to handle. Furthermore, these steps are illustrated in detail in figure 1. To make the simulation code more effective, a single matrix a can be created to embody the combined effect of these two matrices, as expressed in the following equation.

$$\textbf{ROT1} \times \textbf{ROT2} = \begin{pmatrix} \cos\alpha\cos\beta & \sin\beta & \cos\beta\sin\alpha \\ -\cos\alpha\sin\beta & \cos\beta & -\sin\alpha\sin\beta \\ -\sin\alpha & 0 & \cos\alpha \end{pmatrix}$$

The trigonometric expressions necessary for solving the system are:

$$\begin{aligned} \sin\alpha &= \frac{V_{i\,(\text{CM})(Z)}}{\sqrt{V_{i\,(\text{CM})(Z)}^2 + V_{i\,(\text{CM})(X)}^2}} \\ \cos\alpha &= \frac{V_{i\,(\text{CM})(X)}}{\sqrt{V_{i\,(\text{CM})(Z)}^2 + V_{i\,(\text{CM})(X)}^2}} \\ \sin\beta &= \frac{V_{i\,(\text{CM})}}{\sqrt{V_{i\,(\text{CM})(X)}^2 + V_{i\,(\text{CM})(Y)}^2 + V_{i\,(\text{CM})(Z)}^2}} \end{aligned} \tag{2.35}$$

where $V_{i\,(\text{CM})(Z)}$ represents the velocity of the ion along the z-axis in the center-of-mass frame following the collision, $V_{i\,(\text{CM})(Z)}$ and $V_{i\,(\text{CM})(Z)}$ are similar expressions for the x and y axes.

2.5 Application of the null-collision model to the problem

Using the null collision model detailed in section 1.4, equation 1.12 is solved to generate random numbers for the mean free time (τ) of the ion.

$$P(\tau) = \exp\left(-\int_0^\tau \nu dt\right) \sim \exp(-\nu\tau) \tag{2.36}$$

The outcome indicates that the cumulative function does not reach 1, as τ assumes values in the interval $[1, 0]$, which falls within the range of $[0, \infty]$. This discrepancy arises from the null collision model proposed by Skullerud [46], which suggests that some ion collisions do not lead to momentum transfer, leaving the ion's free path unaffected. In this context, a random number is required to determine the collision frequency (ν'). Taking into account null collisions, the artificially generated collision frequency must exceed the actual one (ν). For example, assuming that (ν') is twice (ν), implying that the randomly generated free time (τ') is half of the actual free time (τ), results in an underestimated mean free path, possibly halved. Consequently, it is inferred that half of the simulated collisions are ineffective, while the rest can alter the ion's trajectory through momentum transfer. By generalizing the notion that half of the total collisions are ineffective, one can relate this to Skullerud's approach by considering the time (t) at which the artificially generated collision frequency surpasses the real one. To address this issue, Skullerud expanded his solution to encompass velocity-dependent scenarios. He introduced a constant trial frequency higher than the actual velocity-dependent collision frequency ($\nu(\nu)$), a technique integrated into the simulation algorithm.

We tested the Skullerud method using an example of $\tau(t) = 1$ with a change function of $1 + \sin(2t)$ and a fixed random generated collision frequency in the time interval $[0, 4]$. The random data generated for the free time values of the collisions that will occur in this time interval are filled into

(a) $v' < v$ (b) $v' > v$
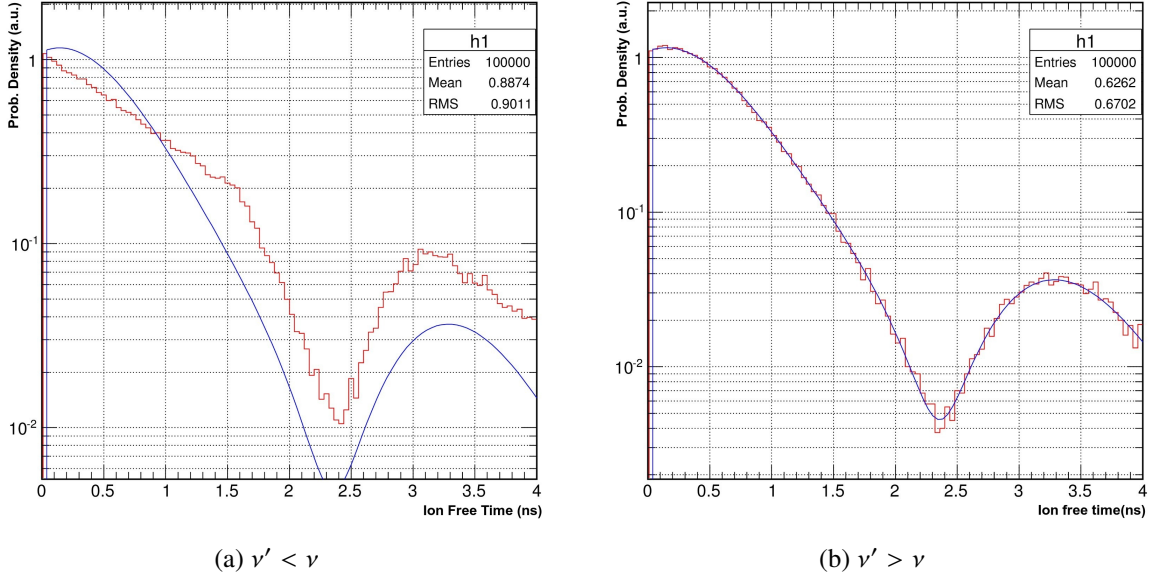
Figure 4. Histograms for the conditions of free paths of ions.

a two-dimensional histogram. The precision of the method was tested by comparing the fit of the histogram with the blue line formed by connecting the points distributed according to the mentioned function. We observed two different outcomes: when the random generated collision frequency value ($v' = 1.1 Hz$) was less than the maximum value of the actual collision frequency value ($v = 2.1 Hz$), the theory could not be verified (figure 4(a)). However, when the random generated collision frequency value ($v' = 3.1 Hz$) was greater than the maximum value of the actual collision frequency value ($v = 2.1$ Hz), the theory appeared to be confirmed (figure 4(b)). This example demonstrates that Skullerud's theory is valid as long as the ($v' > v$) condition is satisfied.

2.6 Free path and mean free path of the ion

The ion's free path refers to the distance it covers without engaging with the carrier gas, and this distance can vary and is contingent on different factors. The average distance an ion travels between collisions is known as the mean free path. To establish a probability distribution for the mean free path, one can consider that if an ion moves a very small distance or a multiple of this distance (a) without any interaction, the derivative's mathematical definition comes into play.

$$f(x + \delta) = (1 - \delta a)f(x)$$
$$f(x + \delta) - f(x) = (1 - \delta a)f(x) - f(x)\frac{f(x + \delta) - f(x)}{\delta} = \frac{-\delta a f(x)}{\delta} \tag{2.37}$$

The mean free path is denoted by the symbol a, thus the solution is $f'(x) = -af(x)$. The probability function obtained by solving this differential equation is expressed as

$$f(x) = e^{-\lambda x} \tag{2.38}$$

The aim of this research is to investigate the influence of ions on gas detectors. To do this, random numbers must be assigned to the physical quantities used in the calculations. The Monte

Carlo method is used to generate these random numbers within the ROOT interface of the simulation program Garfield++ [31]. This section of the study will explain which physical quantity, along with the corresponding physical rule or rules, and how random values will be assigned using a ROOT command line. To generate a random number for a particular physical quantity, a "Probability Density Function" ($f(x)$) must be defined for that quantity. The inverse integral of this function produces a Cumulative Function ($F(x)$). This could lead to the development of a subroutine for the simulation program Garfield++ that takes into account the effects of ions, thus providing more accurate results.

$$F(y) = \int_0^y f(x)dx \tag{2.39}$$

The normalization condition requires $f(\infty) = 1$. Additionally, it is critical to consider the following regulation to randomly assign a value (y) within the interval $(0, 1)$ when expressed by the cumulative function (u):

$$P(u < f(x)) = f(x) \tag{2.40}$$
$$P(u < f(b)) = f(b) \tag{2.41}$$
$$P(\underbrace{F_{\text{inv}}(u)}_{\text{random b}} < y) = F(y) \tag{2.42}$$

3 Results and discussion

3.1 Collisions and scatterings

This study investigates the behavior of ions in gaseous detectors, including the scattering phenomenon. The spectrum of the radial components of the velocity of the ion after the collision is obtained, which reflects the distribution of the radial components of the velocity of an ion that has been scattered along the z-axis after the collision. The symmetry of these components produces a two-dimensional histogram with a disc-like shape.

It is important to note that, except for the highest values, the distribution appears to be mostly uniform, indicating a high level of uniformity. Furthermore, assuming the ion and gas have equal masses, the radius of the disk-shaped histogram, which represents the maximum velocity the ion can attain after the collision, is much smaller compared to the maximum velocity achieved when the mass of the gas atom is 10^{10} times greater than the mass of the ion. The velocity of the ion before the collision remains unchanged after the collision, indicating that if the gas mass is significantly larger, the ion does not transfer momentum or energy. This observation aligns with the principles of physics, which state that when the ion and gas masses are equal, the post-collision velocity of the ion is half of the total momentum. Additionally, when the gas mass is twice that of the ion, the momentum is shared in the same proportion. The computer code developed based on these physical principles has been validated to be consistent with the laws of physics governing elastic collisions.

The characteristics of the two-dimensional histogram with sharp edges need to be explained. When the impact parameter is close to zero, it indicates a head-on collision, resulting in a higher momentum transfer. On the other hand, a larger impact parameter suggests a more tangential collision, leading to a lower momentum transfer and minimal loss of velocity for the ion. The probability of a head-on collision is very low, as evidenced by a probability calculation. Therefore, it is important to

consider the probabilities of different scenarios in order to understand the results of the two-dimensional histogram. In the case of an ion moving along the z-axis and colliding with a stationary gas atom or molecule, the impact parameter is represented as b.

$$b = R \cos \frac{\theta}{2} \tag{3.1}$$

The total radius, R and the scattering angle, θ, are used to transform the distribution of the ratio of the radial components of the velocity after collision (g) to the distribution of velocity (s). To accomplish this, a variable substitution is necessary to express them as functions of one another.

$$s = g(x)$$
$$g(x) = \sin(2 \ \arccos x) \tag{3.2}$$

There are four potential outcomes that can be derived by reversing this function. Nevertheless, two of these results generate negative values, which are not physically permissible since the impact parameter cannot be negative. The two valid solutions are:

$$\frac{\sqrt{1 - \sqrt{1 - s^2}}}{\sqrt{2}}, \qquad \frac{\sqrt{1 + \sqrt{1 - s^2}}}{\sqrt{2}} \tag{3.3}$$

The two directions of the radial velocity component can be expressed mathematically. When the impact parameter is zero, the radial velocity is also zero, which means a head-on collision. Conversely, when the impact parameter is equal to the gas radius, the radial velocity is equal to the gas radius, indicating that the ion merely brushes against and passes through. To calculate the derivative of the function g, a variable transformation must be performed. The derivative can then be calculated as follows.

$$f(s) = \frac{f(g^{\text{inv}}(s))}{|g'(g^{\text{inv}}(s))|} \tag{3.4}$$

The inverse of $g(y)$ has two distinct answers, so it is necessary to consider the combination of these two solutions. This leads to the following conclusion.

$$f(s) = \frac{1}{2} \frac{s}{\sqrt{1 - s^2}} \tag{3.5}$$

Integrating the azimuthal angle eliminates the linear dependence of s. This solution is reflected in the two-dimensional histogram in figure 5, which shows a flat distribution in the center of the disk and sharp changes at the edges.

The graph in figure 6 clearly illustrates the precision of the mathematical solution in explaining the sharp edges of the two-dimensional disk-shaped histogram. The plotted curve is an exact match to the histogram, indicating a perfect fit. The blue lines in the histogram represent the spectrum of the radial velocity distribution, whereas the red lines represent the results obtained from the equation. Note that the histogram is based on the assumption that the mass of the gas is much larger than that of the ion. Until now, experiments have assumed that the gas atom or molecule was stationary. However, it is necessary to take into account the velocity caused by the thermal energy of the gas atom,
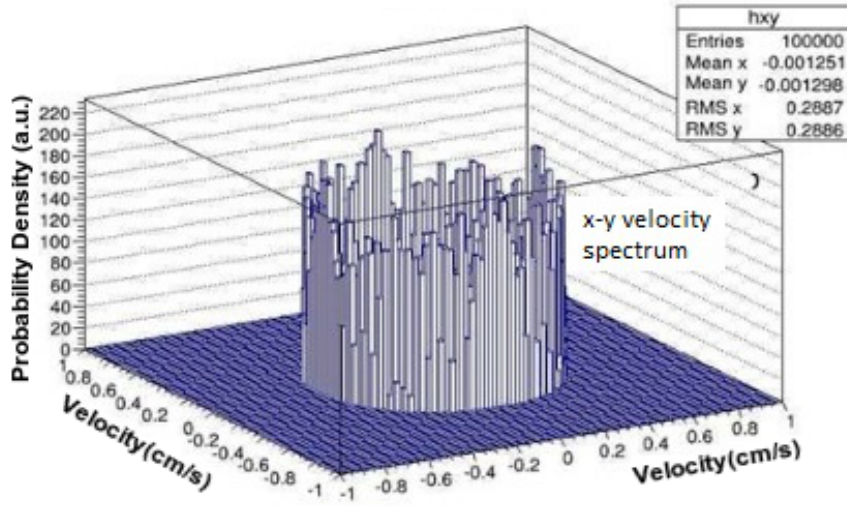
Figure 5. The three-dimensional spectrum of the ion's radial velocity distribution.
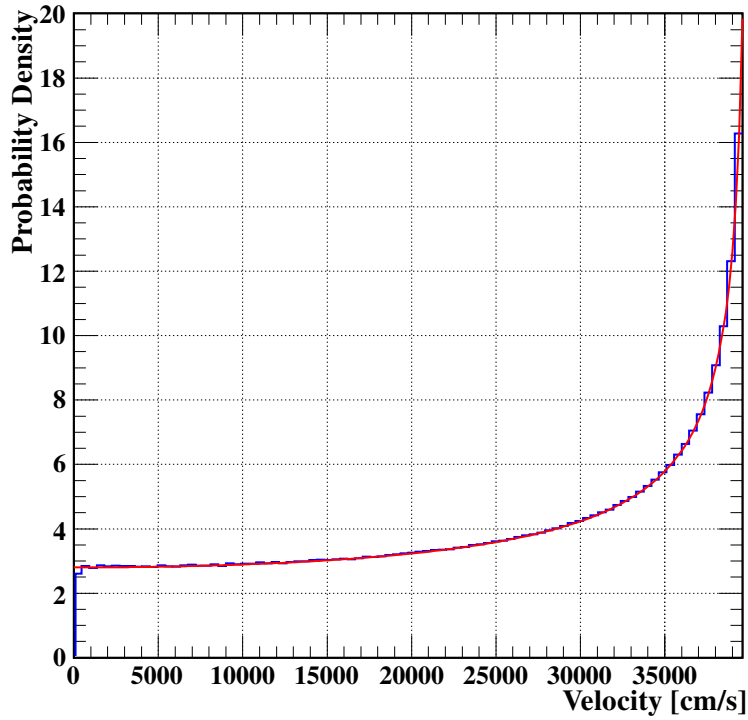
Figure 6. Radial velocity distribution spectrum of the ion.

which follows the Maxwell-Boltzmann distribution for particle velocities. The three-dimensional expression for this velocity is the following:

$$v_{\text{thermal}} = \frac{3k_{\text{B}}T}{m} \tag{3.6}$$

This trial conducted a distribution test on the polar angle, which is the angle of scattering of the ion. Taking into account the same masses for the ion and gas particles, and a temperature of 0 K, it is highly unlikely that the polar angle would be zero due to a head-on collision. The maximum value of the polar angle is $\frac{\pi}{2}$ radians, which indicates nearly tangential collisions, but the probability of this is still very low. As the temperature increases, the velocity of the gas particles colliding with the ion also increases, leading to a higher probability of ion backscattering, which is a scattering angle close to π radians. To compute the distribution under the given conditions, a simulation code was created. The mass of the Ar$^+$ ion was assumed to be equal to the mass of the gas ($6.63 \, 10^{-26}$ kg). The initial velocity of the ion was set at an average of 40000 cm/s, based on data from sources in the literature that are relevant to the given conditions.
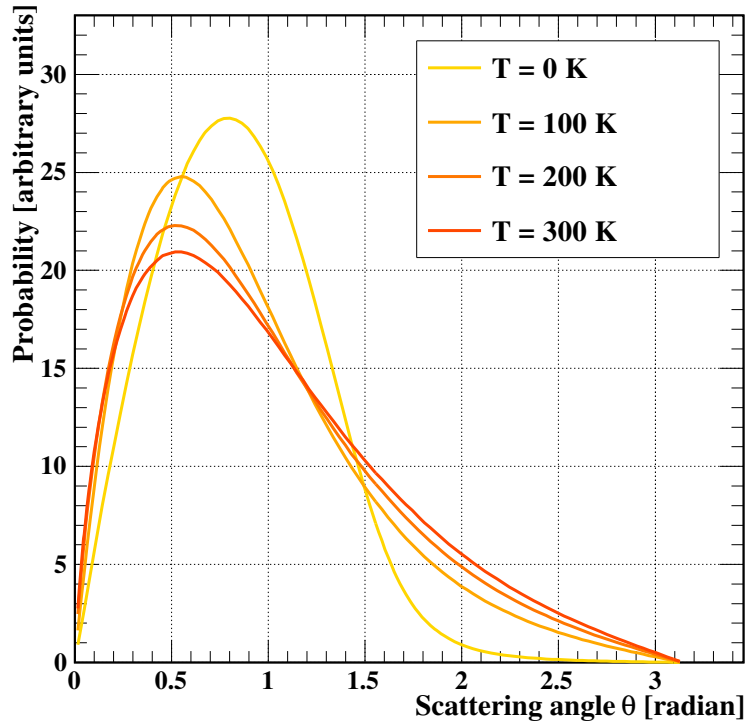

**Figure 7.** Distribution of polar angle for various temperature values.

3.2 Free time for the ion

The frequency at which an ion collides with gas atoms varies over time depending on the electric fields and velocities involved. According to the Skullerud approximation, the collision rate between an ion and gas atoms is solely dependent on time. Nevertheless, empirical studies using a test simulation code with diverse ions under varying electric fields and velocities have revealed that the collision frequency is influenced by multiple physical parameters. The graphs depicted in figure 8 illustrate how the collision frequency of an ion with gas atoms changes with time for different electric fields and velocities.

The parameters of the Ar$^+$ ion were set at a radius of 71 pm [45], a cross section of 615 Mb, a temperature of 300 K, a pressure of 101, 225 Torr, an initial velocity of 5 µm/ns, an electric field of 10^6 Volt/cm, a mass of 37240 MeV, and a charge of 1 elementary charge. It was assumed that the ion's motion was linear. Figure 9 shows the distribution of free times between collisions, which was
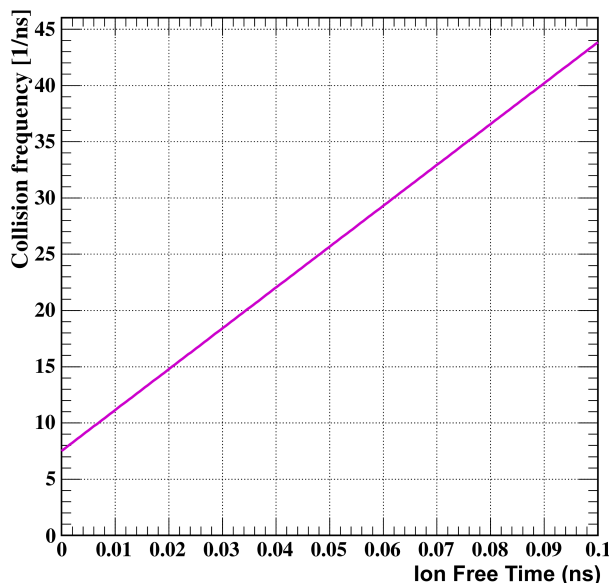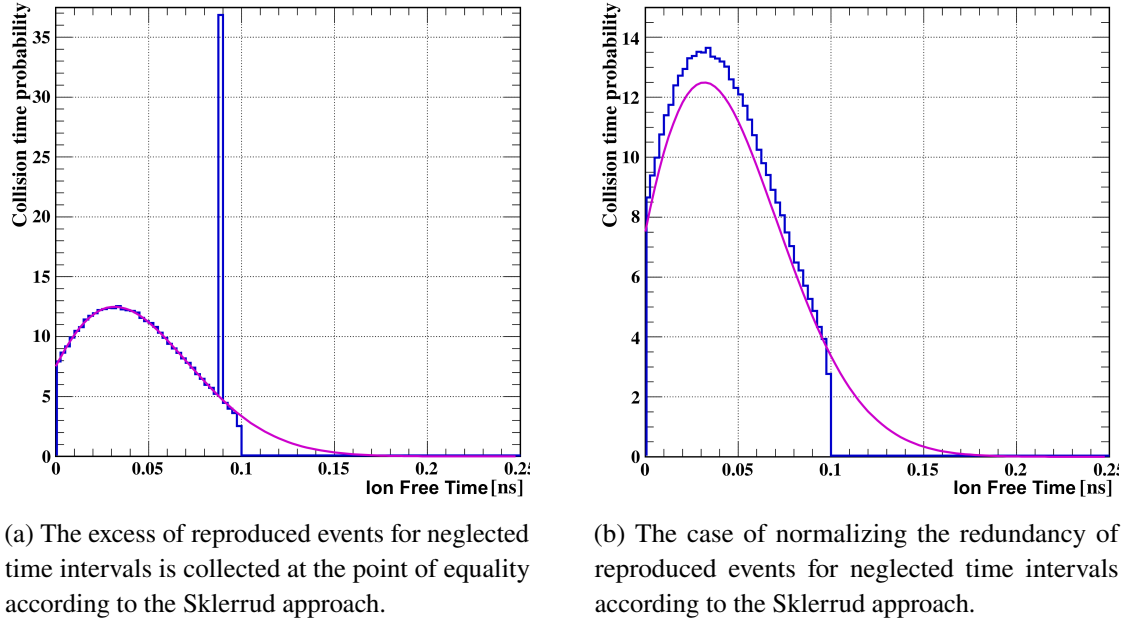
Figure 8. Variation of collision frequency of Ar^+ ions in Argon gas.
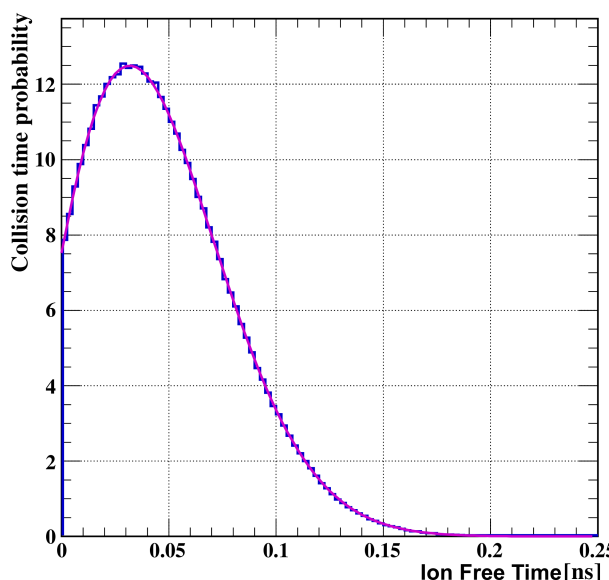
Figure 9. Distribution spectrum of free time of Ar^+ ions in Argon gas.

obtained by the Skullerud method. The relationship between the maximum collision frequency and the collision frequency at any given time was studied. It was found that when the collision frequency of ions with gas atoms is lower than the maximum collision frequency, the process follows the expected pattern. However, when the collision frequency exceeds the maximum collision frequency, ineffective collisions that do not transfer momentum cannot be accurately simulated. To address this issue, two different methods were attempted.

The first technique attempted to replicate the free collision times, yet this led to additional events that caused redundancy, as demonstrated in figure 10(b). The distribution of these extra events did not match the theoretical curve (purple curve) based on the Skullerud approach.

(a) The excess of reproduced events for neglected time intervals is collected at the point of equality according to the Sklerrud approach.

(b) The case of normalizing the redundancy of reproduced events for neglected time intervals according to the Sklerrud approach.

Figure 10. Distribution spectrum of free times of Ar$^+$ ions in Ar gas.

An alternate strategy was used when the maximum collision frequency was less than the instantaneous collision frequency. In this case, the free time was generated by returning to the point where the maximum collision frequency was equal to the instantaneous collision frequency, as seen in figure 10. This showed that if the maximum frequency was calculated within the loop where the free time was generated, the problem could not be avoided. For this research, the maximum collision frequency was set to 40 GHz.

The purple line in the graph represents the results obtained from the simulation code developed in this study using the Skullerud approach, whereas the blue spectrum corresponds to the results obtained from the Monte Carlo approach. Both approaches were tested in a scenario where the mean collision frequency exceeded the collision frequency, with the maximum collision frequency set to 40 GHz.

When the rate of collisions exceeds the maximum collision frequency, the Skullerud technique involves going back to the point of equality and changing the maximum collision frequency accordingly. This method guarantees that the simulation takes into account the collisions that were not considered.

Determining the appropriate increment for the maximum collision frequency is crucial. For example, if we use an increment rate of 1.000001, additional events are generated to replace neglected events, resulting in a peak at the equal point when a total of 10^6 events are generated, as shown in figure 11(a). If the maximum collision frequency is lower than the collision frequency, slightly increasing the maximum collision frequency causes the equality point to shift to the right, leading to the expansion and growth of the undesired peak. However, increasing the number of generated events can mitigate this issue, causing the undesired peak to decrease and eventually disappear, aligning the spectrum with the physical state. This is illustrated in figure 11(b), where events generated by 10^7 with an increment rate of 1.000001 for the maximum collision frequency are shown. It is important to note that the Skullerud approach does not provide a clear definition of the increment rate for the maximum collision frequency. However, this study has developed a method to address this problem and obtain realistic results. The maximum collision frequency was set at 40 GHz.
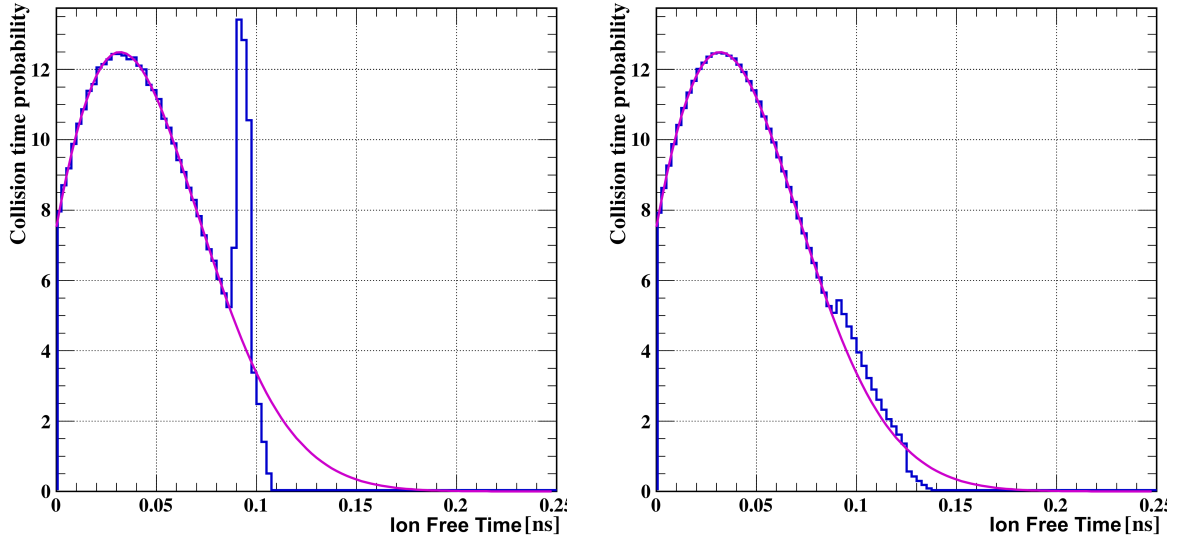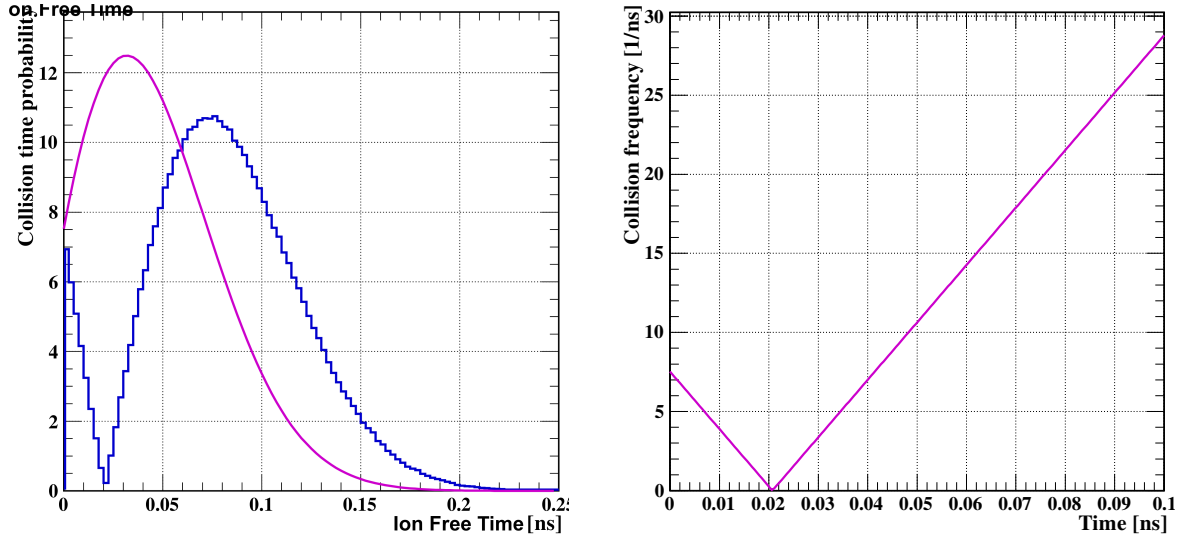
(a) Free time spectrum obtained for 10^6 events generated.
(b) Free time spectrum obtained for 10^7 events generated.

Figure 11. The spectrum obtained when the collision frequency is less than the maximum collision frequency and the rate of increase of the maximum collision frequency is very small (1, 000001).

The spectrum is obtained for collision frequencies that are lower than the maximum collision frequency, with a slight increase rate of 1.000001 for the maximum collision frequency. The left side of the figure displays the spectrum of events in free time generated by 10^6, while the right side shows the spectrum for events generated by 10^7. In this study, the purple lines represent the results obtained using the Skullerud approach, while the blue lines correspond to the spectrum obtained with the Monte Carlo approach. The chosen maximum collision frequency for this spectrum is 40 GHz, with a very small increase rate of 1.000001. The left side of the figure shows the free-time spectrum for events generated by 10^6, while the right side shows the spectrum for events generated by 10^7. This method ensures that the collision frequency accurately reflects the physical conditions, as shown in figure 10. The collision frequency is updated (increased) ($\nu(\tau_{\text{former}})$) for the previous state at an unfavorable moment if the maximum collision frequency at any given instant during the ion's free time interval ($0 < t < \tau$) exceeds the instantaneous collision frequency. This approach guarantees that the collision frequency obtained is consistent with the physical conditions.

The Skullerud method requires the utilization of the absolute value of the magnitude of the velocity of the ion since the collision frequency is dependent on the velocity of the ion, as indicated in equation 3.7. If the ion's velocity is negative, the collision frequency will also be negative, which is not physically feasible. This issue is demonstrated in figure 12(a), where the Monte Carlo simulation (depicted in blue) produces accurate results, while the validation curve obtained using the Skullerud method is incorrectly calculated. The reason for this discrepancy can be observed in figure 12(b), where the frequency plot exhibits a discontinuity. The simulation code utilizes the square of the velocity components, which results in negative velocity values being symmetrically placed with respect to the x-axis. It can be observed that the velocity of the ion remains negative until approximately 0.02 ns, while the maximum point of the curve derived from the Skullerud approximation increases. Therefore, it is crucial to consider the magnitude of the ion's velocity, and thus the simulation code employs the absolute value expression. The results obtained from the code using the Skullerud method

(a) The free time spectrum obtained for the negative ion velocity condition.

(b) Free time distribution spectrum of Ar⁺ ions in Ar gas and variation of collision frequency with time.

Figure 12. Free time distribution spectrum of Ar⁺ ions in Ar gas and variation of collision frequency with time.

are represented by the purple line, while the blue spectrum corresponds to the Monte Carlo approach. On the left, the free time spectrum is depicted for the case of negative ion velocity, while on the right, the time variation plot of the collision frequency is shown for the negative ion velocity scenario.

This equation states that the probability of an ion's free path being equal to or less than a given value is equal to the exponential of the negative of the product of the ion's charge and the electric field strength. This research has hypothesized that the distribution of an ion's free path within a gas environment follows an exponential distribution. To mathematically verify this, the Skullerud equation can be used. This equation states that the probability of an ion's free path being equal to or less than a given value is equal to the exponential of the negative of the product of the ion's charge and the electric field strength.

$$P(t) = \exp(- \int_{t=0}^{\tau} \nu(|v_i + at|) dt) \tag{3.7}$$

The acceleration of the ion is represented by a, and the change in velocity after a time interval t is given by at. Adapting the velocity change within this time period according to the unit system used in the simulation code gives the result.

$$\Delta v = \frac{Ec^2 t(10^{-6})}{m} t \tag{3.8}$$

To finish the proof, two suppositions are brought in. To begin with, it is assumed that the ion is exposed to a steady electric field (E). Second, it is assumed that the ion has no initial speed. These assumptions, although not limited to the proof, are made for the sake of simplicity.

$$P(t) = \frac{N\sigma Ec^2 10^{-6} t}{m} e^{-\frac{1}{2} Ec^2 10^{-6} t^2 \sigma N} \tag{3.9}$$

Neglecting the constants, the probability density distribution can be demonstrated by the following expression.

$$P(t) = te^{-t^2} \tag{3.10}$$

It is possible to mathematically demonstrate that the free path of the ion follows an exponential distribution. To validate this, we obtained the distribution spectrum, which confirms the exponential nature of the distribution. The parameters used for this figure are the same as those in figure 8.
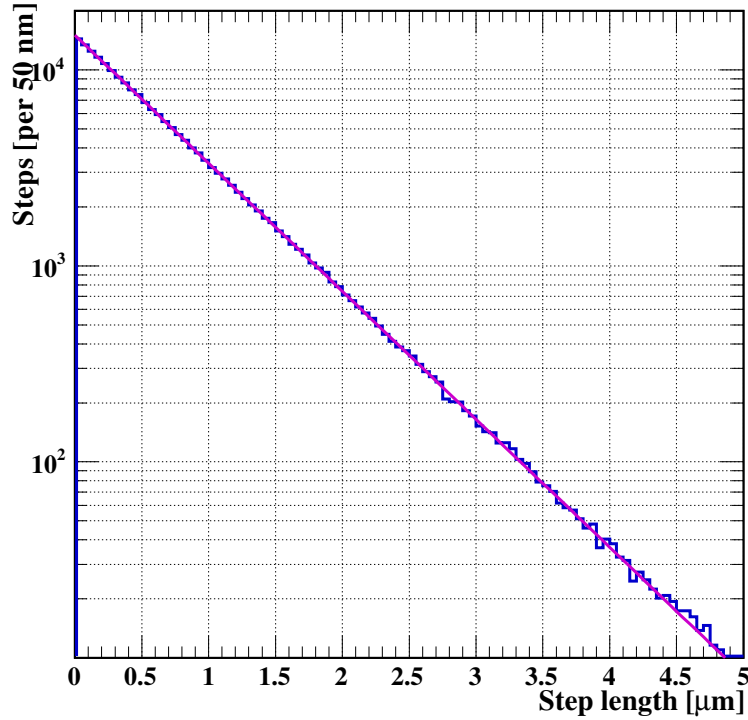
Figure 13. Distribution spectrum of the free path of Ar$^+$ ions in Argon gas.

A more persuasive justification for why the exponential distribution is anticipated for the free path in a gaseous medium is that the likelihood of the free path experiences the following alterations.

$$f(\lambda) = \sigma N e^{-\lambda \sigma N} \tag{3.11}$$

The plot in figure 13 clearly shows an exponential distribution, which confirms the expectation. This implies that the free path of the ion is determined by the number density (N) and the cross section (σ) of the gas. This result confirms what was previously established.

For the purpose of simplifying the analysis, take $f_x(x)$ and $f_y(y)$ as exponential distributions with mean values of λ and μ respectively. This describes the velocity distributions of two gas atoms in a one-dimensional phase space, as illustrated in figure 14.

$$f_x(x) = \frac{1}{\lambda} e^{-\frac{x}{\lambda}}$$

$$f_y(y) = \frac{1}{\mu} e^{-\frac{y}{\mu}}$$
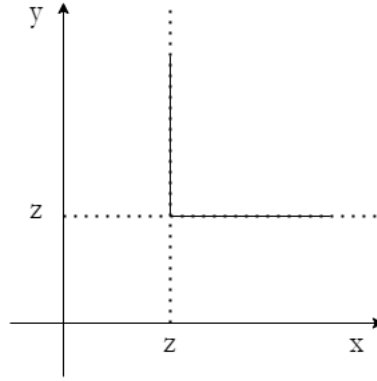
Figure 14. Auxiliary diagram for explaining the method involving obtaining the free time distribution of the gas atom that will carry out the first collision.

We can see that the exponential distribution for z is the minimum of the x and y distributions. By deriving the mathematical expressions and studying the resulting distribution z, we can gain a better understanding of this.

$$f_x(z) \int_z^{+\infty} dy \; f_y(y) = \frac{1}{\lambda} e^{-\frac{z}{\lambda}} e^{-\frac{z}{\mu}} = \frac{1}{\lambda} e^{-z\left(\frac{1}{\mu}+\frac{1}{\lambda}\right)} \tag{3.12}$$

$$f_y(z) \int_z^{+\infty} dx \; f_x(x) = \frac{1}{\mu} e^{-\frac{z}{\mu}} e^{-\frac{z}{\lambda}} = \frac{1}{\mu} e^{-z\left(\frac{1}{\mu}+\frac{1}{\lambda}\right)} \tag{3.13}$$

The sum of the results of the above integrals can be written as

$$\left(\frac{1}{\mu} + \frac{1}{\lambda}\right) e^{-z\left(\frac{1}{\mu}+\frac{1}{\lambda}\right)} \tag{3.14}$$

When we assume that μ is equal to λ, the time of the first collision is found to be half of the average collision time, which is equivalent to the amount of gas atoms present.

If we consider a system with n atoms, the time for the first collision can be calculated by dividing the average collision time by n. For example, in a volume of 1cm^3, there are 2.7×10^{25} gas atoms, making the time of the first collision minuscule. Nevertheless, it is expected to be similar to the average collision time. Moreover, the mean real-time in an environment with n gas atoms can be determined by using the expression for the average collision time of an ion with a gas atom in its surroundings, which is $\frac{\tau}{n}$.

$$\tau = \lambda/v = \frac{v}{(N\sigma)} \tag{3.15}$$

The actual number of gas atoms denoted n, is very large, which means that the average free time is expected to be minuscule. This could lead to confusion as to why the result is much smaller than the average free time reported in earlier studies, since the mean free time is already the time needed for the first collision to take place.

It is essential to take into account that the average free time is an average value derived from a distribution that includes values close to zero. It is quite common for these values to be concentrated around the minimum collision time. Thus, even though the average free time is quite small, it is a normal characteristic of the distribution due to the presence of such near-zero values.

In conclusion, this study has made considerable progress in understanding the behavior of ions in gaseous detectors, particularly by focusing on collisions, scatterings, and free-path characteristics. Through comprehensive simulations and mathematical modeling, we have validated the Skullerud technique for calculating collision frequencies and free paths, guaranteeing that our results accurately reflect physical conditions. Our discoveries demonstrate the importance of taking into account various physical factors such as ion velocity, gas mass, and collision frequency in determining the behavior of ions within gas detectors. The successful application of these methods in our simulations provides a more detailed comprehension of ion interactions in gaseous environments, which is essential for the development and optimization of gas detectors. The knowledge gained from this research not only confirms existing theories, but also opens the door for future progress in the field of particle physics and gas detection technology.

In this study, a novel computational method was developed to investigate the transport characteristics of ions in gas-filled radiation detectors, which are closely linked to the behavior of ions in gaseous detectors. Parameters such as polarizability, mean free path, collision frequency, and mean free time, which directly impact the mobility of the ion, were physically manipulated using the Monte Carlo technique, and the results were validated against fundamental physical principles. As an initial scenario, computations were performed on the drift of Ar^+ ions in an argon environment as a carrier gas. The distribution of the radial velocity components of the ion following an ion-gas collision was represented as a two-dimensional histogram with a disc-shaped pattern, and this result was elucidated utilizing the Maxwell-Boltzmann distribution. The findings regarding the mean free time and mean free path of an Ar^+ ion in an argon carrier gas align with the results derived from Skullerud's methodologies. These findings hold promise for Garfield^{++} simulations, enabling the computation of ion mobility and even cluster ions in the mixture, thereby considering their impact on the detector's gain parameters. The results of this investigation offer novel insights into the behavior of ions within detector settings, significantly enhancing our comprehension of the mobility of ions and its effects on radiation detection efficiency.

4 Conclusion

A novel computational modeling approach utilizing the Monte Carlo method was developed to investigate the ion transport properties in gas-filled radiation detectors. Essential factors affecting ion movement, such as polarizability, mean free path, mean free time, and collision frequency, were examined. The analysis focused on the motion of Ar^+ ions in argon, with the accuracy of the results confirmed through the Maxwell-Boltzmann distribution and compared favorably to Skullerud's techniques. The outcomes have potential implications in Garfield^{++} simulations, enabling the evaluation of ion mobility and the effects of cluster ions on detector gain parameters. This study offers valuable insights into the behavior of ions within detectors, improving our comprehension of ion mobility and its impact on radiation detection efficiency. The research results illustrate the dynamic nature of ions in gas environments, underscoring the significance of understanding ion mobility to enhance gas detector simulations and propel the advancement of more effective detection systems.

Acknowledgments

References

[1] M. Titov and L. Ropelewski, *Micro-pattern gaseous detector technologies and RD51 Collaboration*, *Mod. Phys. Lett. A* **28** (2013) 1340022.

[2] F. Sauli, *Applications of gaseous particle detectors in physics and medicine*, *AIP Conf. Proc.* **342** (1995) 335.

[3] V. Peskov et al., *Development of a new generation of micropattern gaseous detectors for high energy physics, astrophysics and environmental applications*, *Nucl. Instrum. Meth. A* **732** (2013) 255 [arXiv:1305.0719].

[4] W. Blum, L. Rolandi and W. Riegler, *Particle detection with drift chambers*, Springer-Verlag, Berlin, Germany (1994) [DOI:10.1007/978-3-540-76684-1].

[5] P.N.B. Neves, C.A.N. Conde and L.M.N. Távora, *A new experimental technique for positive ion drift velocity measurements in noble gases: Results for xenon ions in xenon*, *Nucl. Instrum. Meth. A* **580** (2007) 66.

[6] G.F. Knoll, *Radiation detection and measurements*, John Wiley and Sons Inc., New York, U.S.A. (2000).

[7] Y. Kalkan et al., *Cluster ions in gas-based detectors*, 2015 *JINST* **10** P07004.

[8] P.M.C.C. Encarnação et al., *Experimental ion mobility measurements in Ar-CO2mixtures*, 2015 *JINST* **10** P01010.

[9] P.M.C.C. Encarnação et al., *Experimental Ion Mobility measurements in Ne-CO2and CO2-N2mixtures*, 2016 *JINST* **11** P05005.

[10] A.M.F. Trindade et al., *Experimental study on ion mobility in Ar-CH4mixtures*, 2014 *JINST* **9** P06003.

[11] A.F.V. Cortez et al., *Experimental ion mobility measurements for the LCTPC Collaboration*, *Nucl. Instrum. Meth. A* **936** (2019) 451.

[12] P. Dwivedi et al., *Gas-Phase Chiral Separations by Ion Mobility Spectrometry*, *Anal. Chem.* **78** (2006) 8200.

[13] H.W. Ellis et al., *Transport properties of gaseous ions over a wide energy range*, *Atom. Data Nucl. Data Tabl.* **17** (1976) 177.

[14] H.W. Ellis et al., *Transport properties of gaseous ions over a wide energy range. Part II*, *Atom. Data Nucl. Data Tabl.* **22** (1978) 179.

[15] H.W. Ellis, M.G. Thackston, E.W. McDaniel and E.A. Mason, *Transport properties of gaseous ions over a wide energy range. Part III*, *Atom. Data Nucl. Data Tabl.* **31** (1984) 113.

[16] L.A. Viehland and E.A. Mason, *Transport properties of gaseous ions over a wide energy range, IV*, *Atom. Data Nucl. Data Tabl.* **60** (1995) 37.

[17] A. Deisting, C. Garabatos and A. Szabo, *Ion mobility measurements in* Ar–CO_2, Ne–CO_2, *and* Ne–CO_2–N_2 *mixtures, and the effect of water contents*, *Nucl. Instrum. Meth. A* **904** (2018) 1 [arXiv:1804.10288].

[18] T. Wyttenbach and M.T. Bowers, *Gas-Phase Conformations: The Ion Mobility/Ion Chromatography Method*, in *Modern Mass Spectrometry*, C. Schalley, ed., Springer Berlin Heidelberg (2003), p. 207–232 [DOI:10.1007/3-540-36113-8_6].

[19] T.R. Marrero and E.A. Mason, *Gaseous Diffusion Coefficients*, *J. Phys. Chem. Ref. Data* **1** (1972) 3.

[20] W.P. Boynton and W.H. Brattain, *Interdiffusion ofgases and vapors*, in *International Critical Tables of Numerical Data, Physics, Chemistry and Technology*, McGraw Hill Book Co., New York, U.S.A. (1929), vol. V, pp. 62–63.

[21] W.A. Roth et al., *Physikalisch Chemische Tabellen*, 5 Auflage, Springer, Berlin, Germany (1923, 1927, 1931).

[22] Y.S. Touloukian et al., *Thermophysical Properties Research Literature Retrieval Guide*, Plenum Press, New York, U.S.A. (1967).

[23] A.A. Westenberg, *Present status of information on transport properties applicable to combustion research*, *Combustion and Flame* **1** (1957) 346.

[24] A.A. Westenberg, *A Critical Survey of the Major Methods for Measuring and Calculating Dilute Gas Transport Properties*, in *Advances in Heat Transfer Volume 3*, Elsevier (1966), pp. 253–302 [DOI:10.1016/s0065-2717(08)70053-4].

[25] R.H. Perry et al., *Chemical Engineers' Handbook*, 4th Edition McGraw-Hill Book Co., New York, U.S.A. (1963), Chapter 14, pp. 19–23.

[26] N.B. Vargaftik, *Manual of Thermophysical Properties of Gases and Liquids*, FM, Moscow (1963), pp. 603–631, in Russian.

[27] K.B. Bischoff and D.M. Himmelblau, *Survey of Mass Transfer*, *Ind. Eng. Chem.* **56** (1964) 61.

[28] K.B. Bischoff and D.M. Himmelblau, *Mass Transfer*, *Ind. Eng. Chem.* **57** (1965) 54.

[29] D.M. Himmelblau and K.B. Bischoff, *Mass Transfer*, *Ind. Eng. Chem.* **58** (1966) 32.

[30] K.B. Bischoff and D.M. Himmelblau, *Mass Transfer*, *Ind. Eng. Chem.* **60** (1968) 66.

[31] R. Veenhof, *Garfiel Simulation Program* (2010).

[32] P. Langevin, *Une formule fondamentale de theorie cinetique*, *Ann. Chim. Phys.* **5** (1905) 269.

[33] B.K. Chatterjee and R. Johnsen, *An estimating formula for ion–atom association rates in gases*, *J. Chem. Phys.* **93** (1990) 5681.

[34] Y. Itikawa, *Cross Sections for Electron Collisions With Carbon Dioxide*, *J. Phys. Chem. Ref. Data* **31** (2002) 749.

[35] E.A. Mason and H.W. Schamp, *Mobility of gaseous Ions in weak electric fields*, *Annals Phys.* **4** (1958) 233.

[36] L.A. Viehland and C.C. Kirkpatrick, *Relating ion/neutral reaction rate coefficients and cross-sections by accessing a database for ion transport properties*, *Int. J. Mass Spectrom. Ion Process.* **149–150** (1995) 555.

[37] E.W. McDaniel and E.A. Mason, *The mobility and diffusion of ions in gases*, John Wiley & Sons, New York (1973).

[38] E.A. Mason and E.W. McDaniel, *Front Matter*, in *Transport properties of ions in gases*, Wiley-VCH Verlag GmbH&Co. KGaA (1988).

[39] E.A. Mason, *Ion mobility: its role in plasma chromatography*, Plenum Press, New York, NY, U.S.A. (1984), pp. 43–93

[40] H.E. Revercomb and E.A. Mason, *Theory of plasma chromatography/gaseous electrophoresis. Review*, *Anal. Chem.* **47** (1975) 970.

[41] G.A. Eiceman and Z. Karpas, *Section 2: Mobility of Ions in the Gas Phase*, in *Ion Mobility Spectrometry*, Second Edition, CRC Press (2005), pp. 39–66.

[42] MATLAB version 7.10.0, The MathWorks Inc., Natick, MA (2010).

[43] A. Sharma and F. Sauli, *Low mass gas mixtures for drift chambers operation*, *Nucl. Instrum. Meth. A* **350** (1994) 470.

[44] R. Brun and F. Rademakers, *ROOT: An object oriented data analysis framework*, *Nucl. Instrum. Meth. A* **389** (1997) 81.

[45] M. Winter, *The periodic table on the web* (2010), http://www.webelements.com.

[46] H.R. Skullerud, *The stochastic computer simulation of ion motion in a gas subjected to a constant electric field*, *J. Phys. D* **1** (1968) 1567.

[47] R.E. Johnson, *Introduction to Atomic and Molecular Collisions*, Springer Science & Business Media (2012) [DOI:10.1007/978-1-4684-8448-9].

[48] B.M. Smirnov, *Physics of Ionized Gases*, Wiley (2001) [DOI:10.1002/9783527617708].

[49] J. Tian, P. Chai, Z. Sun and H. Ouyang, *An azimuthal mode detection method based on angular deviation and its application in compressor*, *Measurement* **213** (2023) 112712.

[50] U.H. Ramadhani, D. Lingfors, J. Munkhammar and J. Widén, *On the properties of residential rooftop azimuth and tilt uncertainties for photovoltaic power generation modeling and hosting capacity analysis*, *Solar Energy Advances* **3** (2023) 100036.

[51] D.J.G. Marques et al., *Dual-Polarity Ion Drift Chamber: A new system to measure the mobility of positive and negative ions*, *Nucl. Instrum. Meth. A* **1029** (2022) 166416.

[52] T. Ikeda et al., *Development of a negative ion micro TPC detector with SF_6 gas for the directional dark matter search*, 2020 *JINST* **15** P07015 [arXiv:2004.09706].